SAND2007-5432C

LASER MICRO SPIN FORMING*

Paper # P 542

D.O. MacCallum[(1)], J. A. Palmer[(1)], Roman, G. A. [(2)]
[(1)] Sandia National Laboratories, Albuquerque, NM 87185
[(2)] University of Florida, Dept. Mech. Eng., Gainesville Fl

Abstract

Laser forming has been shown effective as a non-contact bending technique for 0.15 mm thickness cantilever beams made from Neyoro G, a high-strength, high-reflectivity, high thermal conductivity material. The current work reports on efforts to extend laser forming to miniature 3-D axisymmetric shapes from similar thickness originally flat discs.

In conventional spin forming, a rotating sheet metal disk is formed over a shaped mandrel by a mechanical tool. In preliminary experiments performed on both cold-worked and annealed discs of 0.127 mm thick 304L stainless steel, a scanned laser beam replaced the spinning apparatus. A scan head steered ~25W of laser power (1.064 µm) onto the disc. A laser-based sensor was incorporated to measure surface movements.

Temperature and surface displacement measurements are compared to FEA modeling results. Laser powers, beam trajectories, temperature gradient changes and bend results for single and multiple passes will be presented.

Finally, the information developed was used to design a micro forming apparatus (MFA), which was then assembled and tested. Motor speeds and control methodologies, mandrel-collet-tailstock-carrier design considerations, and beam scanning path geometry concerns will be discussed. CAD renderings of the system, along with the final assembly, will be shown.

Introduction

Previous work in laser contact forming showed that laser bending of thin parts was feasible [(1)]. It was demonstrated that first, ~200 µm total deflection ranges could be obtained and second, that deflections on the order of 10-50 µm are possible for the extremely thin, high strength, highly reflective and conductive parts studied.

This work extends that idea to laser spin forming where a laser is substituted for the mechanical tool normally used in the process.

While an appropriate motor, controller, mandrel, tailstock and motor mount were being designed and built, (Figure 14), an set xy-scanning head was used to steer a 25W, continuous wave, flashlamp pumped, ND:YAG laser beam onto a stationary thin disc in preliminary experiments on 304SS discs at various laser and beam speed parameters.

Experimental

Laser Bending Using Beam Scanning Head

The setup used is illustrated in Figure 1. The laser was mounted outside a commercial micro-machining cabinet and the beam brought to the processing space using 6 turning mirrors before the final aperture to the scan head. The final focusing lens (114 mm f.l.) is between the output of the scanner and the part.

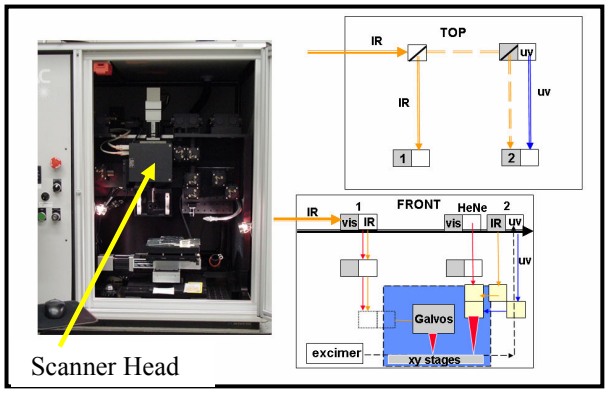

Figure 1: Process Space and beam path to scanner head.

The laser (configured for TEM_{00} mode operation) is capable of delivering ~25W continuously, with a 14 mm raw beam diameter at maximum power. There is some loss, ~ 4 W, through the multiple turning mirrors due to absorption of the beam on multiple, AR (anti-reflective) coated surfaces. The real loss of

the beam turns out to be the aperturing effect of the scanning mirrors themselves. This turned out to be problematical and will be discussed in detail later.

The scan head's maximum travel without spherical aberration (Figure 2) ~ 40 mm (+/- 20 from "0") but they will steer the beam considerably further: ~ 100 mm (+/- 50 from "0"). The laser beam diameter at the lens was measured to be ~ 10mm and its diameter at the part ~ 0.5mm The scanner lens system's scale factor for linear travel deflections and for speed values was different from the nominal (as entered in the controlling computer software) values and needed calibrating. Figure 2 shows the process area of the operating x-y dimensions, and the measured versus specified geometrical (circles and boxes) figures used for calibration. The outer squares are visibly distorted.

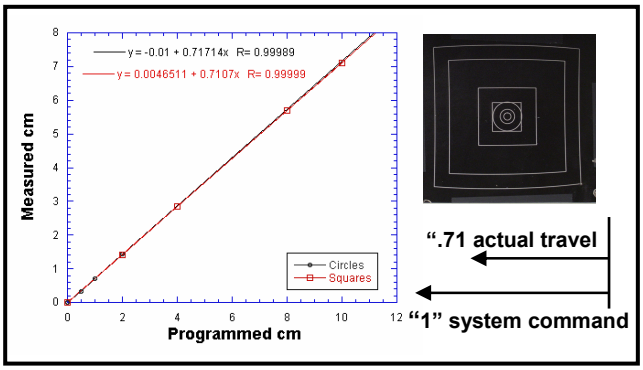

Figure 2. Spherical aberrations limit the beam travel and scale distance and velocity calibrations.

The slope of the curve gives scale factors of 0.717 cm and 0.712 cm for the circle and box shapes, respectively. Therefore, a 1 cm travel will go ~0.71cm and a 1cm/s velocity will equate to ~0.71 cm/s. This must be taken into account and the conversion calculated ahead of time when programming the motion control. Speeds noted hereafter refer to actual speed and distance values.

Speed was found to be linear over a 0 to 500 cm/s range, using a 3mm diameter circle as the calibrating feature; this was where most of the following temperature and bending experiments were carried out.

The laser, as previously mentioned, is capable of delivering 25 W average maximum power. Measurements (using a Molectron, Model PM-1K water-cooled power meter) determined that only 8 W maximum was reaching the part (Figure 3). After careful alignment and adjustment of the optical path, it was discovered that although the input aperture *to* the scanner head was a 20 mm diameter (for a 14mm raw beam at 25W output power) the galvo internals (mirrors, etc.,) imposed a 10mm aperture to the beam – hence, 40 % of the beam was being lost, accounting for the 12 W of lost power (~ 4W are lost through the multiple mirror optical track previously mentioned).

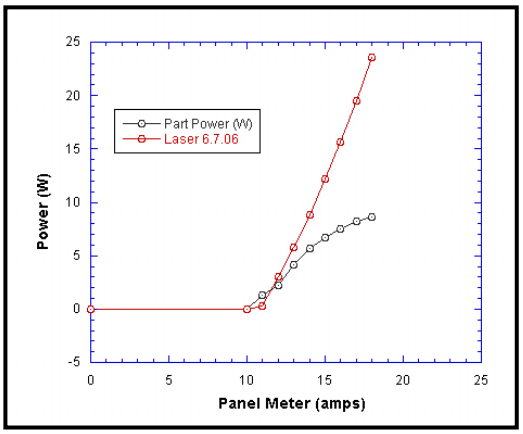

Figure 3. Laser power loss due to internal aperturing of scanner head.

The reason the power curves match at the lower end is that the raw beam varies in size, dependent on the average power, from thermal lensing[2] (shape distortions at the output end of the laser rod due to thermal heating during the pumping and lasing process of a flashlamp-pumped laser resonator) and the multi-mode operation of the laser resonator. Though the resonator was tuned to be near TEM_{00}, there are still longitudinal modes that contaminate the desired gaussian distribution that cannot be removed. At the lower end of a few watts the raw beam is on the order of 10mm and fits the internal aperture well; as the power increases, thermal lensing increases the divergence angle of the beam, which increasingly overfills the galvo aperture, throwing away an increasing amount of the beam. This can be seen in the asymptotic behavior of the "part power" curve in Figure 3.

The maximum power used to process the parts was restricted to 8W. This gave minimal bending; enough to indicate the process direction (bending towards the beam) and that more total bend angle would result from higher incident power. 8W was used to carry out the following laser bending experiments.

Bending Experiments

Bending experiments and thermal characterization was done on two types of samples: 304SS punched

from shim stock and 304SS annealed, chemically etched parts. The punched discs measured ~6 mm in diameter and 0.127 mm thick; the etched discs measured 5.95 mm diameter by 0.127 mm thick, and averaged 0.0283g/disc (punched discs were not weighed) in mass.

The etched discs were purchased from a commercial manufacturer and were made from 304SS stock. They were chemically etched with a low pH, $FeCl_3$ solution, water rinsed and alcohol dried. They are "flat" with minimal residual stresses, compared to the punched samples, which started with a very slight saddle shape from the shearing process.

A sample holder was made in a flat Al plate 8.9 mm thick, with a 6.15 mm diameter hole bored 0.70 mm deep (and maintained flat) to support the part, keeping it centered but not clamped, beneath the processing beam.

Bending Experiments – Punched 304 SS Material

Several of the stamped material parts were run using 8W laser power and 0.71 cm/s beam velocity to determine the bending direction. It was found that in all cases the punched material bent (concave) towards the laser source. Through experimentation, it was found that a circular, 0.3 cm diameter beam path gave consistent results. Bending of up to 2mm was observed; however, due to inaccuracies in the concentricity of the part relative to the beam path and residual stresses in the punched part or from the process itself, the bending was not homogeneous, but gave saddle shapes, accentuating the starting -- very slight -- out-of-plane shape.

Bending Experiments – Etched 304 SS Material

Samples were the manufactured 304 SS discs, chemically etched from annealed material, and were flat. Runs were done at 2, 6, and 8 W laser power at various scan speeds: 3.6, 7.1 and 71 cm/s. No shield gas was used and the samples were mounted in the bored out holder, unclamped. The beam trajectory diameter was 0.35 cm, and the parts were cycled 1 – 3 times. Total bend (still concave towards the laser beam) was much less than the punched parts, especially at the higher speeds. Only at .71cm/s was some bend (<< 0.1 mm total) seen to occur, although it was difficult to measure. Notably, the FE model discussed later indicated that at this power and speed, the total bend would be on the order of 4μm after a single cycle. The etched 304SS will require greater power to induce the correct thermal gradients. A new 45 W fiber laser intended for this use will be discussed.

Thermal Experiments

To characterize the thermal environment of the processed part, and to provide validation information to the modelers, some parts were processed with thermocouples in place. The thermocouples used were shielded, type K, 0.005" diameter, and resistance welded in place. The parts were processed at 8W, ~ 0.35 cm diameter process trajectories, and 0.71 cm/s linear velocity.

Figure 4 shows the locations, top and bottom of the thermocouples superimposed with the part geometry and the beam path (indicated in red) and Figure 5 is an example data set used for analysis, including an "as mounted" view of the thermocouple placements.

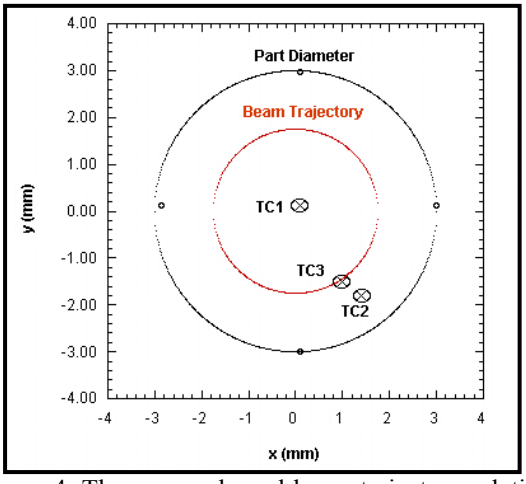

Figure 4. Thermocouple and beam trajectory relative positions. 3.5 mm trajectory on 6 mm part. TC1 is center-bottom; TC2 is edge-bottom and TC3 is edge-top.

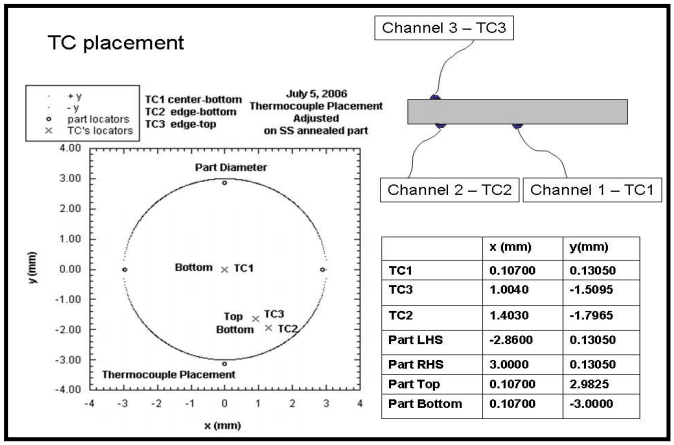

Figure 5. A typical data set with measured values and side-view of the thermocouple set up as provided to the modelers.

Figure 6 shows an overall data set showing multiple traverses and the temperature and gradient excursions seen.

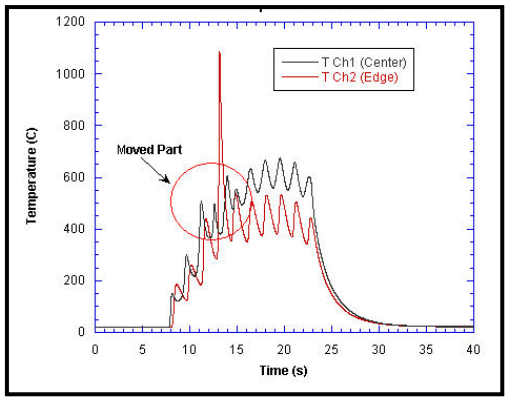

Figure 6. Multiple passes with beam steering on a 3.5 mm diameter trajectory on a 6 mm sheared 304 SS disc. Type K, 0.005" thermocouples. 8W, linear speed ~ 0.71 cm/s.

Thermal Experiments – Punched, Stamped 304 SS Material

Figure 6 shows a detailed view of one of the thermal runs. The data was collected from a single run where the beam completed 11 circuits of the part. The "spike" occurred when the part was moved manually during the run to better align the center with the beam trajectory. Later experiments (especially on the annealed parts) ran only 3 circuits. It can be seen that the average temperature of the part reached ~400 C during the first 2-3 circuits and reached ~600 C only after many cycles. There was no active heat sinking, and no shield or cooling gas was applied. The part was merely placed (unclamped) on an Al plate with through-holes drilled for the lower thermocouples to pass through to the data acquisition system.

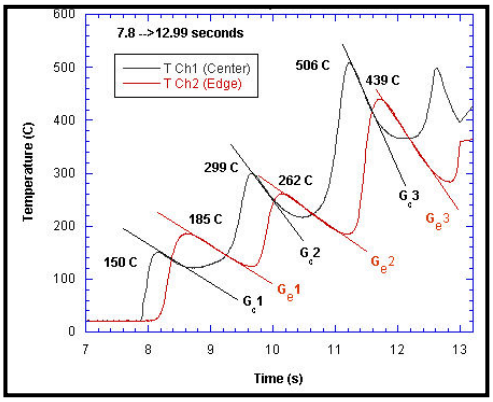

Figure 7. Gradient shifting of sample shown in Figure 4. 8W, linear speed ~ 0.71 cm/s.

Figure 7 examines the time/temperature behavior in greater detail. One can see that the cooling rate as the beam passes the thermocouple location at the center of the part starts out ~the same as, but eventually becomes steeper, than at the outer edge of the part. The thermal gradient experienced at each cycle ~ doubles with each cycle (~25, 50, 100 C/s) for three circuits of the beam.

As noted, it took 6-7 cycles to reach a steady temperature. More laser power is needed to more quickly raise the temperature so that the bending mechanisms can operate for more effective total bending [3,4].

Thermal Experiments – Etched 304 SS Material

Figure 8 is a representative circuit within a data set collected from one of the etched samples. Runs were done at 2, 6 and 8W at 0.35 cm beam trajectory diameter and 0.71 cm/s scan speed. An additional run at 8W, 0.35 cm beam trajectory diameter, with a higher speed of 3.6 cm/s is shown for comparison in Figure 9.

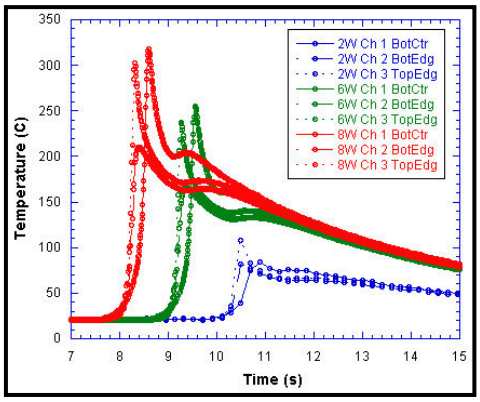

Figure 8. Etched 304SS disc, three thermocouples; 2, 6 & 8W, 3.5 mm trajectory diameter at 0.71 cm/s linear velocity (1 circuit).

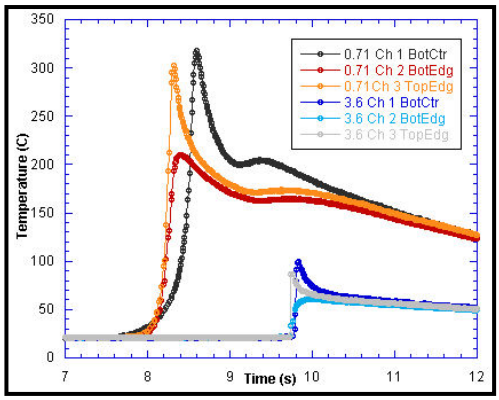

Figure 9. Annealed 304SS disc, three thermocouples, 8W, 3.5 mm trajectory diameter, 0.71 & 3.6 cm/s linear velocity (1 circuit).

The slower speed sample reached a maximum temperature of ~ 300 C, while the faster speed sample reached ~ 100 C maximum temperature. The faster speed was not capable of bringing the surface temperature to a high enough value to induce plastic deformation, at this power level.

Computer Modeling Validation

Numerical simulation of stress, displacement and temperature was performed using Calagio, [5] a nonlinear FEM code employing temperature dependent material properties. Data obtained from thermal measurements was used to validate the computer model, which was then used to visualize the thermal gradients obtained in the material under these processing conditions and to calculate displacements and stresses.

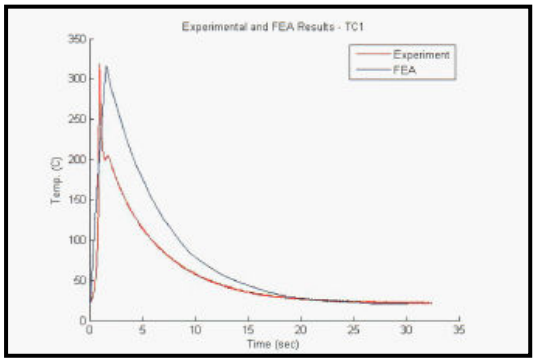

Figure 10. Experimental vs. FEM temperature curve. TC 1 located center-bottom.

A circular piece of sheet metal was modeled and meshed for the FEA using a 6 mm diameter and a thickness of 0.127 mm. The model and mesh were computationally dense in the annular region where the laser beam spot rotates about the center. The laser heating of the sheet metal is modeled as an applied surface heat flux boundary condition in these simulations.

Figures 10 and 11 show the calculated temperature history at a location compared to experimental data under similar conditions: TC 1 located center-bottom and TC 3 edge-top.

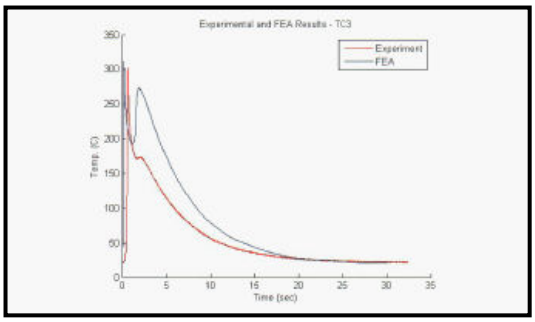

Figure 11. Experimental vs. FEM temperature curve. TC 3 located edge-top.

In Figure 10, the plot shows that the peak temperature is in good agreement. The predicted thermal response of the circular sheet metal does not cool off as quickly as observed in the experiment. In addition, Calagio fails to capture the second peak of the temperature history curve, which has a lower magnitude than the first peak. The temperature comparison between prediction and measurement obtained from TC-3 (Figure 11) also shows good agreement with the peak temperature. The magnitude of the second peak is over estimated by about 100 ºC. The same overestimate in cooling can also been seen in both figures. This has to do with the difficulties in determining the convective heat transfer accurately. Additional information about the ambient environment conditions during the testing is needed to better formulate the convective heat transfer coefficient [6]. The present calculations use a constant value of 0.01 W/cm^2 K. More work is needed to characterize the convective heat loss and to determine a more reliable and accurate heat transfer coefficient.

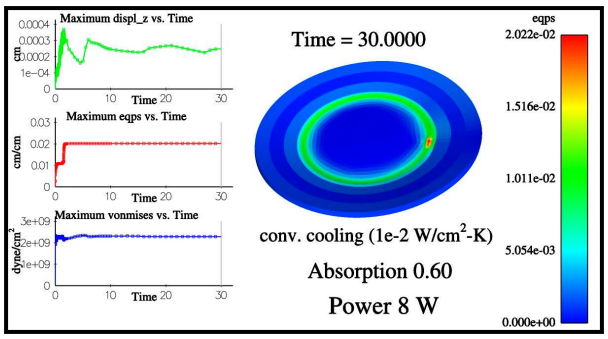

Figure 12. Plastic strain predicted by Calagio FEM .

For any permanent deflection to occur, the induced thermal strain must cause plastic deformation. The plastically strained region, represented by green area, is almost entirely limited to the same area the laser beam traversed. Figure 12 shows the equivalent plastic strain (eqps) at the end of a simulation.

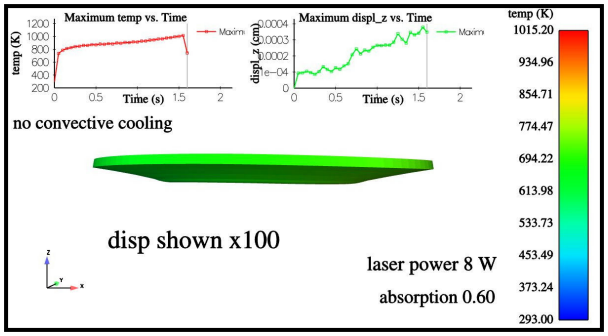

Figure 13. Calagio FEM displacement output.

Total bend in displacement was predicted (Figure 13) to be concave (towards the laser beam) on the order of 4µm after a single cycle. Experimental bend for the same conditions gave << 0.1mm total.

Micro Forming Apparatus Design and Assembly

The MFA consists of a motor, coupler, collet, mandrel, tailstock, and tailstock spring mounted in the motor carrier (Figure 14).

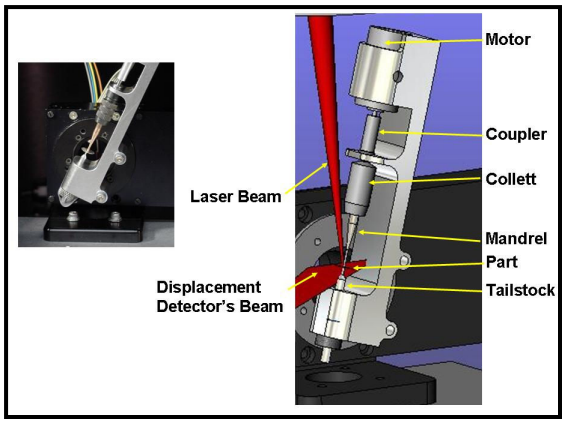

Figure 14. MFA assembly showing input laser process beam and displacement detecting laser beam.

The spinning assembly was mounted to a Newport PR50 high speed rotary stage capable of 20º/s rotation with 0.01º resolution, computer controlled with a SMC100CC single axis motion controller (Figure 15).

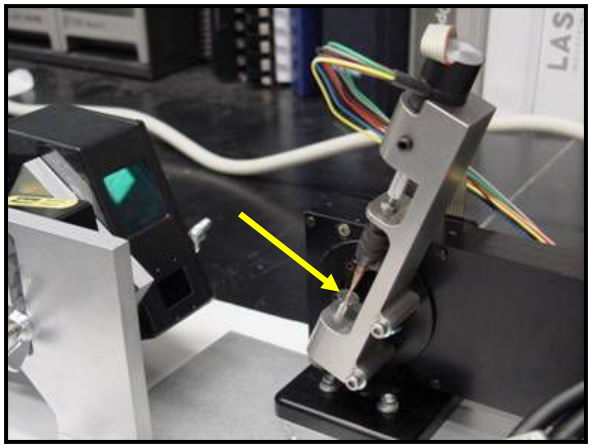

Figure 15. MFA in tilt motor mount with distance detector mounted to the left. Arrow shows the part (6 mm diameter disc) mounted between mandrel and tailstock.

This is used to tilt the motor/carrier assembly during operation and to access the tailstock when mounting/removing parts and, most importantly, to align the part-plane at the optimum angle to allow the maximum beam cone angle to not interfere with the part (as discussed below).

The rotary stage was mounted to an adaptor plate along with the laser displacement detector. The adaptor plate was mounted in the Micro-joining station, directly beneath the scanning head and lens assembly (Figures 1 and 16).

A laser displacement detector was purchased and installed to track a spot on the part to determine the amount of bend as the process proceeds. The detector incorporates a Class IIIa 650 nm laser at 4.8 mW to illuminate the part with a 70 µm spot and 0.2 µm resolution. The beam is reflected from the part back to a sensor on the detector and data is processed at up to 20 µs/point sampling rate. The instrument has a working range of 15 mm within a working distance of 65 – 95 mm (80 mm mid-range). The detector is controlled by computer using the manufacturer's software.

The displacement detector was initially used for validation purposes, and was expected to function as the sensor for a closed-loop feedback control to adjust laser power or spot position on the part during the bending process. The entire MFA assembly was mounted beneath the scanning head as shown in Figure 16.

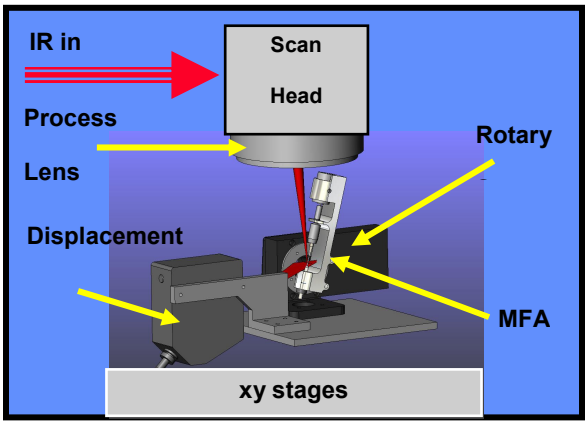

Figure 16. MFA detail relative to input process beam and scan head. See Figure 1 for overall placement.

The motor/controller consists of a brushless d.c.-servomotor capable of 33,000 r.p.m., and a 2-quadrant servo-amplifier with an encoder option for low speed operation. Speed calibrations are shown in Figure 17. Motor speed was measured and calibrated with a Hall sensor connected to an oscilloscope, giving 3 pulses per revolution (cycle). The top speed is ~33,000 rpm and can be modified to go down to a few 1000 rpm with the inclusion of a feedback circuit.

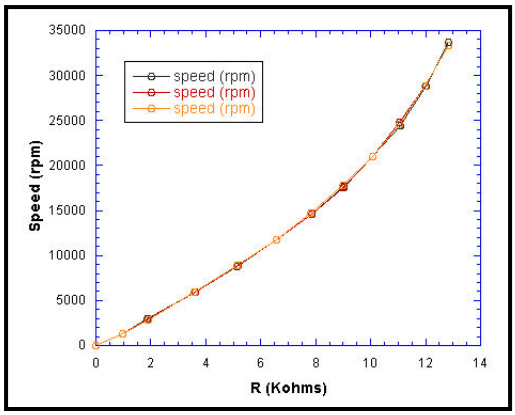

Figure 17. Speed calibrations for motor. 3 replicates.

As noted, the scanner beam's maximum displacement without spherical aberration (recall Figure 2) is ~ 40 mm (+/- 20 from "0"). However, the beam can be deflected considerably further: ~ 100 mm (+/- 50 from "0"). The laser beam diameter at the focusing

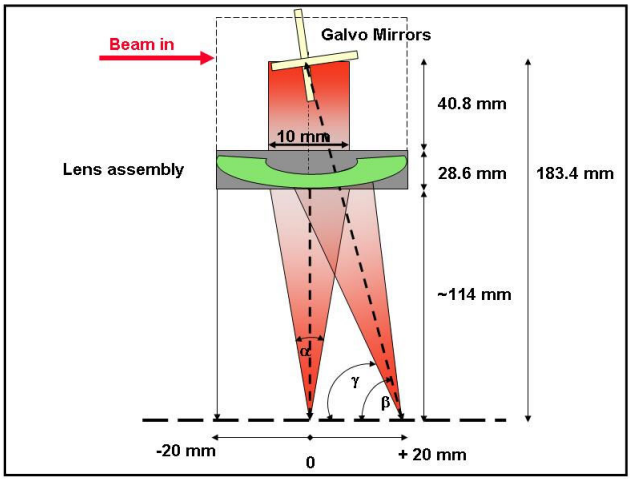

Figure 18. Beam envelope and central ray angles for the motor housing and mandrel dimensions. The critical design parameter is the central half-angle β – ½ cone angle, or $\gamma = 81.5$ degrees.

lens was measured to be ~ 10mm and its diameter at the part ~ 0.5mm. The cone angle of the beam (Figure 18) was determined to be $\alpha = 5$ degrees; with the beam's central ray angle β at maximum aberration-free travel (~20 mm) from "0" to be 84 degrees. The critical design parameter for the motor housing (to avoid impingement from the processing beam) and mandrel dimensions is the central half-angle β – ½ cone angle, or, $\gamma = 81.5$ degrees.

Figures 19 and 20 show the intended part movement with the beam superimposed on the initial and final mandrel designs, respectively.

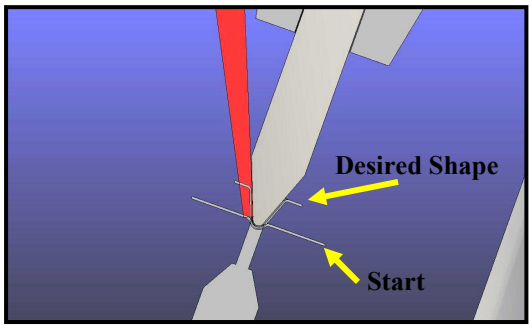

Figure 19. Mandrel impingment with processing beam (original design).

The impact of the previous cone angle analysis showed that the original mandrel design was insufficient, in that the final closure of the part to the

mandrel occluded the beam and would not allow the part to be bent the full range (Figure 19).

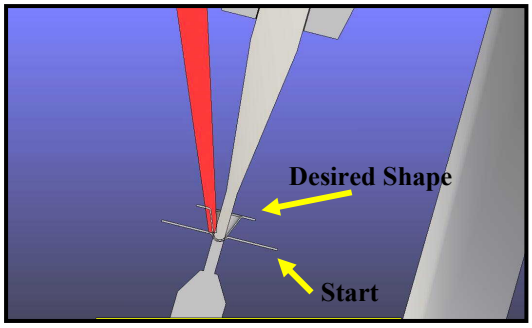

Figure 20. Final mandrel design allows the process beam access, and minimizes bending, flexing and out-of-plane movements.

Figure 20 shows the final design, which allows for a less massive mandrel with the maximum clearance allowed with the existing motor housing.

Figure 21 shows a very schematic overview of the intended process in 2 stages. The preformed part is intended to be temporarily joined to the tailstock, which with the mandrel, is free to spin. The laser would start processing close to the center (Figure 21-left), moving radially outwards and eventually finishing off (Figure 21-right). We do not yet know what the final process path will actually be [4, 7, 8]; but between spinning, tilting and radial displacement, we expect to develop a process which yields a cone.

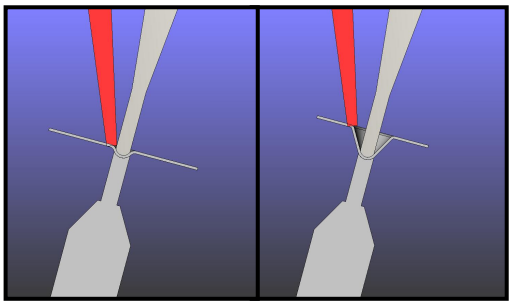

Figure 21. Bending in response to laser beam start to finish – left to right.

The final assembly has been tested, with a part in place (adhesively bonded to the tailstock via a cyano-acrylic glue). Care must be taken when cutting the final length of the retaining tailstock spring: too little length does not compress the tailstock to its correct position; too much puts too high a load on the motor and either slows it down or prevents the motor from turning altogether.

As assembled, the part spins nicely at first, but in a few seconds it "walks" off the rotational axis and is thrown radially outwards. There is some lateral vibration of the mandrel while spinning that needs to be eliminated. Additionally, the tailstock needs some modification to better hold the part in place. Clearly, the concept needs detail development, especially with regards to maintaining concentricity of the mandrel and tailstock.

Discussion

The Thermal Gradient Mode (TGM) [9,10] requires the establishment of a thermal gradient sufficient to induce local inhomogeneous plastic deformation at/near the laser irradiated area. In each step, after cooling, the starting curvature is more pronounced and it is possible that enough curvature and stresses are built up such that subsequent deformations are more susceptible to the Buckling Mode (BM) [11,12], as described by Vollertsen [3]. However, it is expected that the buckling mode would tend to reinforce existing curvature. It is only at the outset, when there is no pre-existing curvature that the system tends to buckle in either direction with equal probability.

Vollertsen concludes that the superposition of TGM and BM does not happen for thin materials (< 1mm thick), which is the case in this work. Our previous work in thin strip bending indicated that rather than creating stresses and strains, stresses or strains are being relieved. We believe (suggested by the increased amount of bending of the punched parts), but have not shown, that although the TGM is not aiding the bending, the mechanism is not a pure BM, and the complexities of the residual stress relaxations of the pre-existing stresses (as pointed out by Vollertsen) probably *do* play a more significant role.

Determining the extent and distribution of initial residual stresses is problematical and further study is needed to assess the robustness of the process parameters to this less determinate starting condition.

Several issues were raised as our MFA Project progressed. The biggest concerns were: heat extraction, the actual shape the material takes during bending, and exploring different mounting ideas of the starting pre-forms.

Heat extraction is extremely important during the entire bending process because bending is not complete until the part returns to ambient; further, localization of the strain requires a substantial thermal gradient. To do this properly, heat must be removed quickly to cool the part and create a thermal gradient. Helium gas blown over the part as the laser

heats it has been suggested to allow for sufficient heat extraction.

Putting the current setup aside, an alternate option is to use the scan head itself as the rotational source, as in the validation experiments. At 250cm/s linear rate, the scan head can deflect the laser beam up to 47000 rpm for a 1mm diameter circle or half that for a 2mm diameter circle (the maximum galvo deflection is about 20 mm). Thus, using the galvos to rotate the laser beam around the part opens up several new possibilities for mounting the pre-form. One simple and logical way is to create a mount (Figure 22) similar to that currently used in the 304SS punched disc experiments.

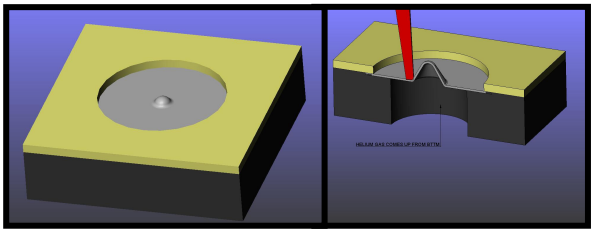

Figure 22. Possible fixturing change for beam steering processing of static part with improved cooling.

A new 45W cw fiber laser (air-cooled, λ = 1091 nm) was purchased that has a smaller, better quality raw beam (5.4 mm diameter and M^2 = 1.09) that should allow greater travel speeds.

Summary and Future Work

Building on previous work involving laser bending of thin, high-strength, high-reflectivity, high thermal conductivity materials, laser micro spin forming was introduced and examined, in feasibility, using a laser scanner head. Bending experiments were described including the laser, scan head and sample parameters and properties for 304SS in both a) punched and b) annealed and chemically etched samples.

Thermal experiments were conducted at conditions that gave the best bend to accumulate data used to validate a FEM non-linear numerical simulation of stress, displacement and temperature, using temperature dependent material properties. This model was then used to visualize the thermal gradients obtained in the material under these processing conditions and to calculate displacements and stresses. The data showed good agreement with peak temperature predictions and bend direction. The magnitude of the cooling rate, and hence, the magnitude of the bend was underestimated due to the difficulty in accounting for convective heat losses during the process.

A new Micro Forming Apparatus (MFA) was introduced, and its design (including motor, coupler, collet, mandrel, tailstock, and tailstock spring and motor carrier), assembly and mode of operation discussed. Use of a laser displacement detector and high speed rotary stage for part and assembly alignment and sensing was introduced and discussed.

MFA detail relative to the input process beam and scan head was shown, along with a discussion of the laser beam envelope and central ray angles for the motor housing and mandrel dimensions. The critical design parameter for this laser and scanner head combination was found to be γ = 81.5 degrees, where γ is the angle necessary to avoid impingement from the processing beam.

Consequences of this analysis on mandrel and processing beam impingment were discussed, including drawings of initial and latest mandrel designs. The latest mandrel design allows the process beam access to the part, and minimizes bending, flexing and out-of-plane movements.

Future work will require study of the process parameter space response to the initial residual stresses state. Additionally, heat extraction, cooling rates and further sample mounting ideas will be explored. A new 45W cw, 1091 nm fiber laser with a smaller, better quality raw beam (5.4mm diameter and M^2 = 1.09) will be employed.

Acknowledgements

Sandia is a multi-program laboratory operated by Sandia Corporation, a Lockheed Martin Company, for the United States Department of Energy's National Nuclear Security Administration under Contract DE-AC04-94AL85000. The authors would also like to thank Michele Steyskal, Rosa Montoya, and Juan Romero, at Sandia National Laboratories.

References

1. D.O. MacCallum, G.A. Knorovsky, J. A. Palmer, J. D. Arvizu, "Precision adjustment of spring contacts using laser forming", ICALEO 2006

2. L. Migliore, "Laser Materials Processing" p 80, ©1996, Marcel Dekker, Inc.

3. Hennige, T., Holzer, S., Vollertsen, F., Geiger, M, "On the working accuracy of laser bending ", Journal of Materials Processing Technology 71 (1997), pp 422-432.

4. Arnet, H., and Vollertsen, F, "Extending laser bending for the generation of convex shapes", Proc. Instn. Mech. Engrs., Vol. 209, pp 433-442.

5. Calagio is a FEM code that uses the SIERRA computing environment to combine thermal analysis and quasi-mechanics codes, Calore and Adagio, respectively, both developed at Sandia National Laboratories Engineering Sciences Center.

6. Casalino, G., Ludovico, A. D., "Optimization and modeling of laser forming of stainless steel circular sectors", Journal of Laser Applications, Vol 15, No. 2, May 2003.

7. Hennige, T., "Development of irradiation strategies for 3D-laser forming", Journal of Materials Processing Technology, 103 (2000), pp. 102-108.

8. Kin, J., Na, S.J., "Development of irradiation strategies for free curve laser forming", Optics and Laser Technology 35 (2003), pp 605-611

9. Vollertsen, F., "An Analytical Model For Laser Bending", Lasers in Engineering, 1994, Vol. 2, pp. 261-276.

10. Yau, C.L., Chan, K.C., Lee, W.B., "A New Analytical Model for Laser Bending", Proc. LANE '97

11. Vollertsen, F., Komel, I., Kals, R., "The laser bending of steel foils for microparts by the buckling mechanism – a model ", Modelling Simul. Mater. Sci, Eng. 3 (1995) 107-119.

12. Magee, J., Watkins, K. G., and Steen, W. M., "Advances in Laser Forming," Journal of Laser Applications, vol. 10, no. 6**,** pp. 235-246, 1998.